Kyvelou, P., Kyprianou, C., Gardner, L. and Nethercot, D. A. (2019) Challenges and solutions associated with the simulation and design of cold-formed steel structural systems. Thin-Walled Structures. 141, 526-539.

CHALLENGES AND SOLUTIONS ASSOCIATED WITH THE SIMULATION AND DESIGN OF COLD-FORMED STEEL STRUCTURAL SYSTEMS

P. KYVELOU*, C. KYPRIANOU, L. GARDNER and D.A. NETHERCOT

Department of Civil & Environmental Engineering, Imperial College London, SW7 2AZ, UK

Emails: pinelopi.kyvelou11@imperial.ac.uk, constantinos.kyprianou08@imperial.ac.uk, leroy.gardner@imperial.ac.uk, d.nethercot@imperial.ac.uk

*Corresponding author

Abstract. The treatment of cold-formed steel sections in design codes is very largely restricted to individual members under ideal conditions. More efficient design is possible if the complexities of the structural response caused by the thin plating and complex shapes, together with the actual conditions of load introduction and restraint arising from practical situations can be recognised. Traditionally this has only been possible by resorting to full-scale testing. This is, of course, time consuming and expensive; moreover, the impossibility of covering all variations of all the important problem parameters means that developing a comprehensive understanding of all aspects of the physical behaviour is unlikely. Numerical analysis offers the promise of an alternative approach. However, for this to be reliable there must be confidence that it accurately models the physical situation. For the past decade a programme of research has been underway aimed at the provision of a more complete understanding of the structural behaviour of cold-formed steel sections when employed in particular practical situations. Three such cases are addressed herein: purlins as used in the roofs of industrial buildings, beams used to support floors and columns forming part of a stud wall framing system. In each case the process has been to firstly identify all the important structural components including fastening arrangements, then to develop numerical models using ABAQUS that represent each of these physical features to a sufficient degree of accuracy, then to validate the models by comparison with all available test data, then to conduct parametric studies covering the full range of variables found in practice and, finally, to use the pool of results and the improved insights into behaviour as the basis for improved design approaches that, by more accurately capturing the key physical features, provide better predictions of performance. An important feature of this has been to ensure that the resulting design procedures were the simplest possible consistent with reliable predictions.

Keywords: cold-formed steel; flooring systems; numerical modelling; purlin systems; stud walls

1 INTRODUCTION

Cold-formed, light-gauge steelwork has been one of the most fertile areas for research and development in the field of structural steelwork over the last few decades, leading directly to greatly increased use of these members as primary structural elements. Since the forming process for cold-formed sections allows much greater freedom than is the case for heavier hot-rolled products, considerable ingenuity in cross-sectional shapes has been possible, bringing with it the benefits of more efficient material usage but also the challenge of needing to consider more complex structural response. This arises from two basic properties of the product: the thinness of the plate elements in typical structural shapes and the complexity of the structural behaviour resulting from both this thinness and the greater variety and complexity of shapes possible with the cold-rolling process.

But there is a further element of complication: cold-formed members are rarely used as individual beams or columns but typically form part of a more complex structural system in which the interaction of the various components, including the fastening arrangements, results in significantly better performance than would be predicted by considering the single member acting on its own. Initially, this behaviour could only really be investigated through the costly and time-consuming full-scale testing of suitable assemblies, among the most notable of which were the series of tests on complete clad steel frame buildings conducted by Bryan and Davies in the 1970s and 1980s that led to recognition of 'stressed skin action' in such structures (Bryan, 1973; Bryan & Davies, 1979; Bryan & Davies, 1980; Davies, 1982; Bryan & Deakin, 1989).

More recently the development of powerful and accessible numerical analysis through the development of commercially available software packages such as ABAQUS, ANSYS, SAP etc., has meant that an alternative approach is now possible. However, this needs to be used with care, understanding and intelligence in order that reliable results be obtained. That said, both the depths of insight possible and the range of problems that may be studied are far larger than would be possible if only physical testing were used.

Over the last decade, a coordinated programme of research at Imperial College London - much of it conducted in close collaboration with a major manufacturer of cold-formed steel products - has utilised sophisticated numerical modelling in conjunction with limited laboratory testing to address three areas: purlins, floors and walls. Work in each of these areas has reached different stages. For purlins, comprehensive studies of different practical arrangements have shown far more precisely how different systems behave, allowing for a fresh approach to design that recognises all possible forms of response and which permits the available capacity to be used to the full. The fundamental benefits of treating flooring as a composite system, rather than as isolated beams with load transmitted from the non-contributing floor boarding, have been demonstrated and the basis of a design approach similar to that used for conventional steel-concrete floors, including recognition of partial interaction and partial shear connection, established. Studies of stud wall systems are at an earlier stage but it has already been shown how numerical modelling can accurately represent all the essential features of the physical arrangement and that response that correctly recognises the beneficial interactions between components, is far superior to treatment as isolated members.

For each of the three topics, an essentially similar approach has been followed. This has comprised:

1. A careful appraisal of all available relevant test data aimed at establishing the key physical aspects of the particular problem area. Unfortunately, in a surprisingly large number of cases, the data were found to be unhelpful - usually because of incomplete measuring and/or reporting of essential items but sometimes because the testing arrangements did not replicate the intended practical situation.
2. Assembly of a numerical model using ABAQUS (2013) that includes all the essential physical features identified in step 1. Ingenuity is required in securing a balance between accurately catering for all important effects without introducing undue complexity; features that often prove troublesome include: connections, contact areas and load introduction points.
3. Controlling the numerical/convergence aspects of the solution so as to ensure tracing of post-peak load behaviour. This requires a judicious mix of operating in load, displacement and arc length control, with displacement control being more challenging for distributed loading.
4. Validation of the numerical solutions through detailed comparisons against as much reliable test data as possible. Such comparisons should use several measures of response e.g. key deflections, failure modes, spread of plasticity etc.
5. Generation of a portfolio of numerical results that sensibly cover the practical range of each of the key parameters. In doing this, account should be taken of regions within the design space that will not be practical e.g. where serviceability deflections will govern.
6. Careful appraisal of all the results (including the test data) with the aim of developing an understanding of cause and effect, i.e. which problem variables are most influential, situations in which response is relatively insensitive to changes in certain parameters etc.
7. Identifying a framework for the design approach. This may involve enhancement of existing procedures to include additional features or the adaptation of a method previously used for similar problems or the derivation of a new approach based on the improved physical understanding.
8. Where necessary, refinement of the design approach through extensive comparisons with the numerical and experimental data, including identification of the limits of application. Even though the design approach may be based on sound physical principles, it is important to remember that its validation will only have covered a limited range so it should be made clear that application outside this range may well be inappropriate without further validation.

The following sections illustrate the application of the above general principles to three different structural arrangements that employ cold-formed steel members acting in conjunction with other structural elements. In several cases, it has been necessary to conduct subsidiary experimental or numerical studies to ascertain the behaviour of these items. More complete descriptions of these and other features of each of the three programmes of study may be found in the references to detailed aspects of each provided herein.

2 PURLIN SYSTEMS

Cold-formed steel purlins, which are frequently employed to support the roof cladding of industrial buildings, are typically designed as individual members rather than as components

of a more complex structural system. As a result, the benefits arising from their interaction with other components of the same structural system are often ignored (i.e. cold-formed steel sheeting, support cleats etc.), leading to inefficient designs.

Furthermore, when two-span arrangements of purlins are employed, their design is simply based on the principles of elasticity, with the ultimate load-carrying capacity of the system corresponding to the bending moment at the internal support reaching the cross-sectional resistance of the purlin, properly reduced to account for loss of effectiveness. On the other hand, the assumption of simple plastic hinge behaviour would not be realistic since the slender nature of the thin-walled purlins, making them susceptible to local instabilities, would both restrict their moment capacity and limit the amount of rotation they can undergo after attainment of their cross-sectional resistance. However, whilst the application of plastic design would lead to unsafe capacity predictions, there remains scope for moment redistribution developing within these systems, recognition of which could lead to substantial performance improvements.

An extended numerical investigation has been carried out at Imperial College London in order to investigate the structural performance of two-span purlin arrangements, with continuity being achieved either by purlins of double-length continuous over the central support or by connecting two different purlins over the central support by employing a sleeve or by overlapping them – see Figure 1.

2.1 Modelling Challenges

Sophisticated finite element (FE) models were developed in ABAQUS (2013), aiming to replicate the structural behaviour of purlins, taking into consideration their interaction with the constituent components of the roof. The developed models included initial imperfections and accounted for geometrical and material nonlinearities. Some modelling challenges that were encountered during this process are presented herein.

2.1.1 Interaction with the profiled sheeting

The profiled sheeting attached to the top flange of the purlins has a significant influence on their structural behaviour and thus its presence cannot be neglected. However, its direct numerical simulation was found to render the finite element models numerically unstable and computationally inefficient due to the large contact areas. This problem was overcome by omitting explicit modelling of the sheeting in favour of replicating its interaction with the top flange of the purlin through the use of a two-spring model introduced by Hui et al. (2016) and shown in Figure 2. The adopted two-spring model comprised:

(i) A linear spring, located at the position of the physical link between the purlin and the sheeting, to simulate the local restraint offered by the fastener.

(ii) A nonlinear, ‘compression-only’ spring, located at the lip-to-flange junction, preventing upward but allowing downward deflections, to replicate the restraining effect of the sheeting on upward deflections of the purlin flange.

The vertical deflections of the second nodes of the springs were equated to the deflections of the web-flange junction (see Figure 2), to prevent their activation due to global bending of the purlin. The stiffness of the springs was chosen based on a previously conducted sensitivity

study (Haidarali & Nethercot, 2011), to ensure effective restriction of distortional buckling without artificially increasing the local buckling strengths. Finally, the out-of-plane deflections at the web-flange junction (along axis 1 of Figure 2) were restrained, replicating the restraining effect of the sheeting on lateral deflections of the top flange of the purlin. Note that the bending stiffness of the sheeting was not taken into consideration.

2.1.2 Boundary conditions at the supports

Although the aim of all physical tests is to realistically replicate the boundary and loading conditions used in practice, it is often inevitable that some simplifications will be made to facilitate practicality and overcome restrictions arising within the environment of a structural laboratory. One of these simplifications relates to the support conditions of cold-formed steel purlins.

Since, in physical tests, it is common practice for the purlins to simply rest on the support plates of the experimental setup, many numerical models reported in the literature adopt the same layout, with all boundaries applied to the bottom flange of the purlin (Haidarali, 2011). However, in practice, purlins are supported by cleats connected to their web, corresponding to all restrictive boundaries being applied to the web of the member, through its connection to the cleat.

Hence, in order to more realistically replicate the support conditions of the modelled purlins while avoiding explicit modelling of the cleat geometry, shown in Figure 3(a), to keep the finite element model numerically stable, the boundary conditions presented in Figure 3 were adopted. As shown in Figure 3(b), the cleat was modelled as a rigid flat plate, tied to the web of the purlin at the positions of the bolts. Vertical and out-of-plane displacements as well as rotation around the longitudinal axis were restrained at all nodes located at the bottom edge of the rigid plate while nonlinear springs have also been employed, allowing the bottom part of the purlin to move freely away from the cleat but preventing lateral deflections into the cleat.

To investigate the influence of the two alternative sets of boundary conditions, single-span purlins were numerically simulated and, after validation against experimental results reported in the literature (Hui et al., 2016), parametric studies were conducted covering a wide range of cross-sectional dimensions, all of which were examined under both support conditions (i.e. boundary conditions imposed at the bottom flange of the purlin and as shown in Figure 3).

The obtained results are presented in Figure 4, where the ultimate moment capacity of each system M_u is normalised by its equivalent yield moment M_{el} and then plotted against the cross-sectional slenderness $\overline{\lambda}_{cs}$. It can be observed that, although for stockier sections the location of the boundary conditions does not influence the ultimate capacity of the system, with increasing slenderness, application of the boundary conditions at the bottom flange of the purlin leads to substantial underestimation of the load carrying capacity due to premature failure at the supports.

Likewise, a numerical investigation into the structural behaviour of two-span purlins showed that realistic replication of the support conditions allows for the development of lateral torsional buckling in the internal support region, a phenomenon which would otherwise be artificially restricted. As shown in Figure 5, under increasing load, the bottom

flange of the purlin at the internal support of a two-span system deflects laterally, being restricted only at the point where its connection with the cleat is modelled.

Hence, it is obvious that the way boundary conditions are modelled can have a significant influence on the ultimate load carrying capacity of the system as well as on the exhibited failure modes; suitable consideration must be therefore given to ensure realistic modelling of the support conditions while being computationally efficient.

2.1.3 Solver scheme and loading setup

An important feature of the finite element models for continuous purlins was that they be able to follow post-peak load behaviour so that the delivered levels of rotation capacity could be compared with those needed to permit the necessary degrees of moment redistribution to occur.

Hence, for the numerical analyses of single-span and two-span continuous purlin systems, in order to track the post-peak response of the system, the modified Riks solver (Riks, 1979), which is based on the Newton-Raphson method, was employed as this is the most appropriate solver scheme for static problems with geometrical and material nonlinearities (Schafer et al., 2010; Hui et al., 2016).

However, for the numerical investigation of two-span sleeved and overlapped purlin systems (presented in Figure 1(b) and 1(c), respectively), the adaptive automatic stabilisation scheme was employed. The reason for this choice lies in the highly unstable behaviour of cold-formed steel members arising from their thin-walled nature, making them prone to local instabilities (i.e. local and distortional buckling) as well as in the wide contact surface between the two overlapping purlins along the internal support region, rendering the Riks solver unable to reach the peak system load or trace the post-ultimate response of the system.

Several researchers have compared numerical results obtained using automatic stabilisation and arc-length (Riks) solution schemes when analysing cold-formed steel members (Ortiz, 2018; Hui, 2014; Schafer et al., 2010), showing that the two methods yield similar results, provided that the ratio of the energy dissipated by viscous damping to the total strain energy of the system is sufficiently low and that sufficient iterations prior to the peak load are enforced; at least 40 successful iterations before the peak load were ensured for all the analyses presented herein while the ratio of the energy dissipated by viscous damping to the total strain energy of the system was below 0.5%.

One challenging limitation of the stabilisation algorithm that occurred from a modelling point of view is that it can be only used in conjunction with displacement control (ABAQUS, 2013). As a result, the use of a pressure load along the length of the purlin, which had been previously employed in combination with the Riks solver scheme, was no longer an option. This difficulty was overcome by modelling a five-tier whiffle tree beam system, shown in Figure 6, approximating with high accuracy a uniformly distributed load (Hui, 2014). The whiffle tree system was modelled with B31 linear beam elements (ABAQUS, 2013), which were assigned a high stiffness - by setting an artificially high value of the Young's modulus - to avoid excessive bending deformations while the joints between the elements were modelled as pins (*MPC, PIN) to ensure an even distribution of loading along the levels of the whiffle tree and, ultimately, on the purlins.

2.1.4 Connection between purlins for sleeved and overlapped systems

The connection of two purlins at the central support of two-span systems comprises either a short inverted length of purlin (i.e. a sleeve) bolted to both purlins in sleeved systems or one purlin inverted relative to the other, with the two purlins overlapping and being bolted together in overlapped systems. Accurate modelling of the connection between the two purlins at the central support is critical in order to realistically replicate the rotation capacity of the support region which would control the capability of the system for moment redistribution.

Hence, the connection between the purlins was modelled by means of nonlinear spring elements, located at the position of the bolts – see Figure 7. Their assigned load-deformation response was adopted from an analytical model (Ho & Chung, 2006), which had been derived based on experimental data of bolted connections obtained from lap shear tests (Ho & Chung, 2004). The in-plane and longitudinal displacements (along axes 2 and 3, respectively, as shown in Figure 7) of the connected nodes were controlled by the spring characteristics while their out-of-plane displacements (along axis 1) were equated using the command *EQUATION (ABAQUS, 2013). The contact interaction between the two purlins was modelled using surface-to-surface hard contact with the Coulomb friction coefficient μ set equal to 0.3 in the tangential direction. More details regarding the implementation of the connection between the purlins have been provided by Kyvelou et al. (2018c).

2.2 Validation of Developed Finite Element Models

The developed finite element models were validated against experimental results reported in several different literature sources, comprising tests on single and two-span purlins of bare, sleeved and overlapped arrangements. The developed models were found capable of accurately capturing the exhibited failure modes as well as the load-displacement curves of the examined systems – see Figure 8. A summary of the obtained results in terms of the mean FE/test moment capacity and coefficient of variation (COV) for each set of tests is presented in Table 1. The overall validation results indicate good agreement of the numerical predictions with the test data with minimal scatter.

2.3 Observed Structural Behaviour of Purlins

Following development of sophisticated finite element models, and after their validation against all suitable data reported in the literature, parametric studies were conducted to investigate the feasibility of moment redistribution developing within the examined two-span purlin systems (Hui et al., 2016; Kyvelou et al., 2018b; Kyvelou et al., 2018c). The use of finite element modelling allowed the numerical investigation of a wide range of systems, many of which had never been physically tested before. As a result, structural behaviours that had not been previously reported were observed. The varied parameters comprised the cross-sectional dimensions (controlling the cross-sectional slenderness) and the span of the systems (ranging from 4 m up to 10 m).

For most of the examined systems, redistribution of moments into the span regions did occur, but this was typically accompanied by a reduction in moment at the internal support. Hence, at the peak load of the system, the maximum moment attained within the span region

was found to correspond to the cross-sectional resistance of the purlin under sagging moment $M_{max,+ve}$ while the moment at the support, after having reached a maximum (corresponding to the cross-sectional resistance of the purlin under hogging moment $M_{max,-ve}$), had decreased. The evolution of the support and span moments (M_{sup} and M_{sp}, respectively), together with the load carrying capacity of the system P for a typical two-span purlin system, are plotted against the vertical deflection of the span δ_{mid} and are presented in Figure 9(a).

However, for some overlapped systems of short spans, it was observed that the enhanced capacity in the overlapping region exceeded the higher moment that it attracted due to the system continuity, causing the span moment to become critical. In this case, as shown in Figure 9(b), with increasing load, the moment within the span M_{sp} reached its cross-sectional capacity $M_{cs,+ve}$ before M_{sup} reached its corresponding capacity $M_{cs,-ve}$. Hence, for this type of system, redistribution did not occur, with the system failing while still having an elastic distribution of moments.

2.4 Design Recommendations for Purlins

Based on the results obtained from numerous numerical simulations, a design framework has been established for the design of continuous two-span purlin systems. The devised design method makes direct use of cross-section capacities at key locations, together with a factor to allow for the fall-off in moment at the central support and accounting for the cases where no moment redistribution occurs, hence leading to more efficient designs.

The reduction of the moment at the support at the peak load of the system can be calculated according to Equation (1), which recognises that the degree of redistribution within the system depends on the cross-sectional slenderness $\bar{\lambda}_{cs,-ve}$ as well as on the length-to-depth ratio (L/d) of the purlin:

$$a = \left[0.7\text{-}0.0045\left(\frac{L}{d}\right)\right]\bar{\lambda}_{cs,-ve}^{\left[-0.003\left(\frac{L}{d}\right)-1.4\right]} \leq 1 \tag{1}$$

Hence, for a system with α = 1.0, full moment redistribution occurs with the moment at the support maintaining its maximum value up until the peak load of the system. Following the calculation of alpha α, the ultimate load carrying capacity of the system assuming moment redistribution q_α can be calculated according to Equation (2):

$$M_{cs,+ve} = \frac{\left(q_\alpha L^2 + 2\alpha M_{cs,-ve}\right)^2}{8 q_\alpha L^2} \tag{2}$$

where $M_{cs,+ve}$ and $M_{cs,-ve}$ are the cross-sectional moment resistances under sagging and hogging moment, respectively (both taken as positive) and L is the length of each span.

To account for the span-critical systems when the peak load of the system q_{sp} occurs under an elastic distribution of moments:

$$M_{cs,+ve} = \frac{\left(q_{sp} L^2 + 2\,\frac{16 M_{cs,+ve}}{9}\right)^2}{8 q_{sp} L^2} \tag{3}$$

Overall, the load carrying capacity of the system q_d can be calculated according to Equation (4):

$$q_d = \min (q_\alpha ; q_{sp}) \quad (4)$$

The proposed design framework was assessed against data from numerous numerical analyses and was found capable of yielding accurate capacity predictions for the examined systems. More details regarding the development and validation of the proposed design method have been provided by Hui et al. (2016) and Kyvelou et al. (2018c) and are beyond the scope of the present paper.

3 FLOOR BEAMS

Cold-formed steel joists and wood-based boards are used to form flooring systems that are lightweight and easy to prefabricate, transport and assemble on site. However, although there is potential for composite action arising within these systems, they are currently designed with the cold-formed steel joists being considered as the sole load-carrying components. Thus, in order to investigate the feasibility of composite action developing within these systems, an extended investigation was carried out at Imperial College London during which the behaviour of these systems was investigated by means of physical tests and numerical simulations.

Since it was the first time for these systems to be examined under the assumption of a composite scenario, physical experiments had to precede all numerical investigations to both permit the key physical aspects of their behaviour to be identified and to provide a benchmark against which the finite element models would be validated. Thus, twelve large-scale beam tests on flooring systems of 6 m length were carried out where cold-formed steel sections of two thicknesses were examined and alternative means of shear connection, featuring fasteners and adhesives, were investigated – a typical cross-section is shown in Figure 10. The tested beams were simply supported and subjected to four-point bending; the employed experimental layout is shown in Figure 11. Material and push-out tests were also conducted in order to determine the material properties of the structural components and the load-slip response at the beam-board interface, respectively.

The experimental results showed that the structural behaviour of the examined systems can be substantially improved, with up to 100% increase in moment capacity and 40% increase in flexural stiffness being achieved for the systems with the most substantial shear connection. A detailed description of the experimental investigation as well as an extensive analysis of all obtained results has been given by Kyvelou et al. (2015, 2017b).

3.1 Modelling Challenges

Following completion of the experimental investigation, finite element models had to be built in order to broaden the pool of data and, thus, to investigate in detail all different aspects relating to the behaviour of the examined systems. A detailed description of the developed numerical models, which included initial imperfections and material and geometrical nonlinearities, has been given by Kyvelou et al. (2018); some challenging aspects from a modelling point of view are presented in the following sections.

3.1.1 Gaps between adjacent floorboards

The manufacturing process followed for the production of the floorboards results in gaps between them, rendering them discontinuous longitudinally – see Figure 12(a). Since the conducted physical tests had shown that the influence of these gaps on the flexural stiffness of the system can be significant, modelling of the board as longitudinally continuous was deemed to be inaccurate as important physical phenomena would not be captured.

Therefore, in order to model the gaps between adjacent floorboards, the gap contact elements GAPUNI (ABAQUS, 2013) were employed, which allow for contact or separation of two nodes by closing or opening of a predefined gap with the contact direction fixed in space. A representation of the gap between adjacent floorboards in the developed finite element model is shown in Figure 12(b).

The Coulomb friction coefficient μ for the definition of tangential contact between adjacent floorboards was given a value of 0.3 based on experimental findings reported by Gorst et al. (2003). Finally, since the contact interaction between adjacent floorboards was found to cause numerical instabilities, linear smoothing of the nodal force distribution upon sliding was allowed (ABAQUS, 2013).

3.1.2 Modelling of shear connection

The shear connection employed within a composite system controls the characteristics of the shear interface between the structural components and, thus, the strength, stiffness and overall structural performance of the system; its accurate and realistic replication is therefore crucial. In the conducted experimental investigation, the shear connection was implemented by means of self-drilling screws at several different spacings (corresponding to the type of fasteners currently used in practice), and structural adhesive (epoxy resin) applied at the beam-board interface.

Hence, in the ensuing numerical simulations, the self-drilling screws were replicated with SPRING 2 nonlinear spring elements (ABAQUS, 2013), used for connecting two nodes in a fixed direction, with the load-slip response assigned to the springs being determined according to a model proposed by Kyvelou et al. (2017b) and derived from the results of push-out tests – see Figure 13. Similarly, for the simulation of systems with adhesive applied at the beam-board interface, the same type of nonlinear spring elements, located at 20 mm spacings, were employed while their load-slip characteristics had been also obtained from complementary push-out tests (Kyvelou et al., 2017b).

Finally, it should be mentioned that in ABAQUS (2013), the nonlinear spring behaviour is defined by load-relative displacement pairs of ascending order while, outside the given range, the stiffness of the spring is assumed to be zero – see Figure 13. Thus, for all the conducted analyses, the deformations of all connectors at ultimate load were monitored to ensure that shear failure had not occurred. At the position of each spring, the lateral and longitudinal displacements of both adjoining nodes were controlled by the spring characteristics while their vertical displacements were equated using the *EQUATION command (ABAQUS, 2013).

3.2 Validation of Developed Finite Element Models

Following their development, the finite element models were validated against the experimental results of twelve physical tests reported by Kyvelou et al. (2017b) and were found capable of accurately capturing the exhibited failure modes as well as the load-deflection responses and strain distributions on a cross-sectional level; typical comparisons are presented in Figure 14. In Table 2, the moment capacities $M_{u,FE}$ and flexural stiffnesses $(EI)_{FE}$ obtained from the finite element analyses are compared against the equivalent values obtained from physical tests (M_{exp} and $(EI)_{exp}$, respectively), yielding accurate predictions with minimal scatter (Kyvelou et al., 2018).

3.3 Discussion of Observed Structural Behaviour

Following development of sophisticated finite element models, and after their validation against the obtained experimental data (Kyvelou et al., 2018), parametric numerical studies were conducted with the main varied parameters being the depth and thickness of the steel beam, the spacing of the fasteners and the gap size between the floorboards. The results were examined in the context of gains in flexural capacity and stiffness and the attained degree of shear connection. It was found that the mobilisation of composite action is feasible within the examined systems, being more beneficial for the systems comprising thinner steel sections. Up to 140% increases in terms of moment capacity and 40% in terms of flexural stiffness were achieved for the systems employing the most substantial shear connection. A detailed description of the obtained results has been given by Kyvelou et al. (2018), while some phenomena that were observed due to the employed modelling techniques described above will be discussed herein.

3.3.1 Redistribution of forces within the system

During validation of the developed finite element models, it was found that some physical tests were stopped prematurely, shortly after initial buckling occurred and before the ultimate load was obtained, while the numerical simulations continued beyond this point; a typical example is shown in Figure 15. For these cases, the values of maximum load used for the validation were taken as those when the midspan vertical deflection in the numerical simulations reached the level corresponding to the maximum load of the equivalent physical test.

This type of response comprising two peaks was also met during the numerical investigation which later followed, exhibited by systems with high degrees of shear connection. For these cases, although the occurrence of distortional buckling resulted in a drop in load causing the first peak of the curve, redistribution of forces from the compressions flange of the steel section into the timber board enabled further load to be carried until ultimate failure (second peak of the load-displacement curve) – see Figure 16. However, since it was observed that excessively large deflections at midspan were often required for the second peak to be reached, it was decided that only the first peak would be used for the numerical prediction of the moment capacity of the examined systems.

3.3.2 Influence of gaps between adjacent floorboards

The obtained numerical results showed that increasing the size of the gap between adjacent flooring panels resulted in gradually decreasing moment capacity while the flexural stiffness was found to drop sharply in the presence of even the smallest gap, but then remained essentially constant as the gap size increased. Eliminating the gap (e.g. by applying adhesive at the interfaces between the boards), rather than simply reducing its size, would therefore be required to most effectively exploit the available stiffness.

In addition, the finite element models were found capable of capturing a change in the slope of the load-deflection curve of the system, occurring due to closing of the gaps between adjacent floorboards under increasing load, hence rendering the overall response stiffer – see Figure 17. This effect was found to be more pronounced for systems with thinner steel sections and denser screw spacings since the contribution of the board to the stiffness of the system is more influential in these cases where the effective shear connection enables the boards to become more fully engaged after the closure of these gaps (Kyvelou et al., 2018).

3.3.3 Exhibited failure modes

For the vast majority of the examined systems, failure was triggered by distortional buckling of the compressed top flange of the steel beam developing between fixings, at the most critically loaded cross-section longitudinally. This type of failure was in accordance with behaviour observed during physical testing; a representative example is shown in Figure 18 (a).

However, since use of numerical modelling allowed for a wide range of cases to be looked at, a different type of failure was also observed for some systems comprising steel beams with slender webs and substantial shear connection at the beam-board interface (i.e. a dense spacing of fasteners). For these systems, while increasing composite action led to significant increases in moment resistance, the shear resistance, depending mainly on the web of the steel beam, remained essentially unchanged. Thus, shear failure occurred in their shear spans, as shown in Figure 18 (b).

3.4 Design Recommendations for Composite Flooring Systems

Based on the results of the numerical investigation, a design method was introduced to recognise the composite action arising within the examined flooring systems (Kyvelou et al., 2017). The proposed method, which follows the basic principles of current design standards for conventional composite systems (i.e. steel-concrete), yields accurate predictions of the flexural stiffness and moment capacity of the examined systems, accounting for potential reductions in moment capacity due to shear-moment interaction; more details regarding the derived design rules and their assessment have been presented by Kyvelou et al. (2017).

4 STUD WALLS

The use of light-steel framing has gained significantly in popularity over the past couple of decades, since it offers an attractive alternative for industrial, commercial and, more recently, residential construction. Wall systems comprising cold-formed steel studs, set in tracks and

sheathed with plasterboard, are often found in light-steel frame applications, where they provide an essential component in the weather-tight envelope.

The beneficial influence of the bracing effect of the sheathing on the load carrying capacity of stud walls is well known and frequently taken into consideration in design (Simaan & Peköz, 1976; Vieira & Schafer, 2013; Telue & Mahendran, 2004; Tian et al., 2007). However, although the scenario of composite action arising within stud wall systems, bringing further benefits in terms of load carrying capacity, is evident, no relevant research has been conducted thus far.

Thus, in order to investigate the feasibility of composite action developing within the examined systems as well as the beneficial influence of the bracing effect of the sheathing, a numerical investigation has been initiated at Imperial College London (Kyprianou et al., 2018). Finite element models of stud wall systems have been developed in ABAQUS (2013) and validated against experimental data reported in the literature. Modelling challenges that have been encountered during the development of the numerical simulations are presented herein, while parametric studies into the influence of key input parameters are ongoing.

4.1 Modelling Challenges

Some of the modelling challenges met so far relate to the nonlinear behaviour of the gypsum material and to the pull-through effect of screws cutting through the plasterboard. In order to understand and to be able to model these phenomena, material and pull-through experiments are currently being undertaken at Imperial College London, while explicit numerical modelling of the relevant observed behaviour is underway. Some numerical challenges that have been already encountered are presented in the following sections.

4.1.1 Boundary conditions

One of the most challenging aspects of the numerical modelling of stud walls was the accurate and realistic replication of the end boundaries. The assumption of fixed or pinned end conditions for cold-formed steel columns is common practice since perfect end conditions are easy to model and significantly facilitate numerical convergence. However, since in reality cold-formed steel studs are set in tracks, the assumption of perfect end conditions might yield inaccurate results as the structural behaviour of the studs is expected to be dictated by their actual boundary conditions.

Hence, in order to investigate the validity of the assumption of idealised end conditions, numerical simulations including explicit modelling of the track geometry have been developed. The contact properties between the track and the stud have been accurately defined while the nonlinear behaviour of the stud-track connection has also been modelled. A representation of the stud sitting on the bottom track in the developed finite element models, compared with the actual system as used in practice, is shown in Figure 19.

Since the track positioned at the base of the cold-formed steel column is lying on the ground, its support conditions have been simulated by means of nonlinear translational spring elements, allowing upward but preventing downward movement of the system while the track-to-ground connection, which is in practice implemented by a holding-down anchor bolt, has been simulated as a pinned constraint (applied at the node highlighted in red in Figure 19(b)). The track-to-column connection has been modelled by means of nonlinear springs, as

described in Section 2.1.4, placed at the position of the physical link between the two system components, with the spring characteristics controlling deflections along the transverse and longitudinal directions (axes x and z, respectively, as shown in Figure 19).

Similarly, realistic replication of the boundary conditions of the top track dictated positioning of nonlinear springs along its top surface, allowing downward movement by being freely extensible, but preventing upward movement by being incompressible. Finally, all the deflections of the free ends of the springs were equated and tied to a reference node, located at the centre of the track, to which the axial load was applied. It should be noted that the cold-formed steel column was not tied at any point to the bottom or top track, with their interaction being replicated through the definition of edge-to-surface contact properties (ABAQUS, 2013). Likewise, warping deformations at the column ends were free to develop.

4.1.2 Geometric imperfections

The thin-walled nature of cold-formed steel columns renders them susceptible to cross-sectional instabilities, such as local and distortional buckling, as well as to global instabilities, such as flexural and flexural-torsional buckling, when left unbraced. Thus, initial imperfections that ensure that these modes of buckling are not inhibited were incorporated into the numerical simulations.

Simulation of the imperfections was performed by employing the elastic buckling mode shapes corresponding to local and distortional buckling, identified through the finite strip software CUFSM (Li & Schafer, 2010) and distributed longitudinally using sinusoidal functions with periods equal to their corresponding critical half-wavelengths (Hui et al., 2016; Hadjipantelis et al., 2018; Kyvelou et al., 2018). Regarding the global imperfection shapes, these were introduced using single half-sine and full cosine functions for the flexural and torsional buckling modes, respectively (Zhao, 2016). All the cross-sectional and global buckling modes were then scaled to prescribed amplitudes and superimposed. Typical longitudinal distributions of all buckling mode shapes are shown in Figure 20.

4.2 Validation of Finite Element Models

Following their development, the finite element models were validated against physical tests reported in the literature (Vieira et al., 2011). The tested sections were 93.6 mm deep channels with 42 mm wide flanges and a thickness of 1.86 mm while the employed sheathing comprised OSB boards of 11 mm thickness and plasterboards of 12.5 mm thickness. Numerical simulations conducted thus far have shown accurate replication of the key phenomena observed in physical tests, with the behaviour of the system being closer to the one corresponding to the fully fixed (rather than the pinned) end configuration when the applied load is predominantly compressive. Typical comparisons between physical tests and FE simulations are shown in Figure 21. It should be mentioned that, as shown in Figure 21(a), the test load-shortening curves display an initial nonlinearity which is attributed to gaps between the column and the end tracks and to the rigidity of the rig loading system, whereas, the equivalent curve obtained from the FE models captures the theoretical axial stiffness of the column (EA/L). Further validation studies are underway.

4.3 Observed Structural Behaviour

Parametric studies are currently underway for the investigation of the influence of different types of sheathing and spacing of fasteners on the behaviour of stud wall systems, sheathed on either one or both sides and subjected to several combinations of vertical and horizontal loading. Obtained results thus far indicate that the sheathing has a substantial beneficial influence on the load-carrying capacity over the bare steel column, leading to improvements of up to 100%. The attained gains in capacity are attributed predominantly to the restraint against global buckling modes, while further increases due to closer connector spacing are attributed to a reduction in the wavelength of the distortional buckles and to the mobilisation of composite action between the boards and the column. More details regarding the development of the finite element models and of the results of the parametric studies have been presented by Kyprianou et al. (2018).

5 OBSERVATIONS AND REFLECTIONS

Properly used numerical analysis is a powerful tool for studying the structural behaviour of cold-formed steel members in the sorts of practical situations that involve them functioning as part of a structural system. Design treatments that only deal with the member itself - even when augmented by simple allowances for some bracing effects - clearly fail to capture all important features of behaviour and thus, usually, underestimate their true load carrying capacity. Until recently it was only possible to approach this problem at a system level through expensive and time consuming full-scale testing. Work reported herein − which summarises only certain aspects of a 10-year programme − demonstrates that numerical analysis is both a feasible and a potentially very attractive alternative. However, its use is not straightforward as modelling and control of the model so as to ensure the production of accurate, reliable and properly representative results requires a clear understanding of the physics of the problem, considerable skill in utilising the software and care in appraising the outputs. However, providing the work is conducted in a suitably rigorous, careful and comprehensive manner, its potential to greatly improve the design of such systems is considerable. For each of the three different areas studied, each of which has reached a different degree of maturity, it is possible to state:

Purlins - A quasi plastic approach that recognises all levels of redistribution of moments for continuous, sleeved and overlapped systems can provide increases in load carrying capacity of up to 40%, depending on the overall system slenderness, when compared with conventional elastic design with no significant increase in calculation effort.

Floor beams - Composite action between wood-based particleboards and cold-formed steel beams, transmitted through the screw fastenings that will always be present, can deliver increases in load carrying capacity of up to 140%, depending on the balance of stiffness and strength between the boards and the beams, with the necessary design calculations being very similar to those used in more conventional steel-concrete composite construction.

Stud walls - Although currently less advanced, initial studies have shown that wall sheathing provides considerable restraint against global buckling, as well as some degree of restraint against distortional buckling and some composite action, particularly when the

fastener spacing is reduced; exactly how this may best be incorporated in a suitably simple design approach is presently under investigation.

Based on the experience of the Imperial team it is reasonable to assume that many other structural problems − not just those involving the use of cold-formed steelwork − can be treated in an analogous fashion to the methodology described herein. Several have, of course, already been addressed in a similar fashion. However, the collective experience described herein is offered as a model of the way in which the power of today's numerical techniques and the associated software needs to be used thoughtfully in association with limited laboratory testing in a coordinated fashion if complete and reliable solutions are to be obtained.

6 CONCLUSIONS

Lessons from a 10-year research programme into the behaviour of cold-formed steel members when used in practical arrangements that mean that they are functioning as parts of a structural system have been described. These show the value of approaching the problem in a systematic fashion that first identifies the underlying physical behaviour, then finds ways of modelling the contributions of all the important components, validates this thoroughly against representative laboratory tests and then uses the improved understanding gained from parametric studies, which can now be far more extensive than was the case when testing was the only option, to devise more realistic and more competitive design methods - always bearing in mind that the aim should be to provide methods that only require effort comparable to the use of the status quo.

ACKNOWLEDGEMENTS

Much of the work reported herein has been supported through a long term partnership with a leading UK manufacturer of cold-formed steel products - Ayrshire Metals. Not only have they provided financial assistance but also highly valued practical advice and guidance that has ensured that our work reflects the realities of the practical situations. The contributions of former students Mohammed Haidarali and Chi Hui are gratefully acknowledged.

REFERENCES

ABAQUS Inc. (2013) Abaqus (6.13) [Computer-aided engineering, Finite Element Analysis] Pawtucket, USA.

Bryan, E. R. & Davies, J. M. (1980) Design basis of Zeta purlins: Part 2. University of Salford, Department of Civil Engineering Report. Report number: 80/135.

Bryan, E. R. & Davies, J. M. (1979) Design basis of Zeta purlins: Part 1. University of Salford, Department of Civil Engineering Report. Report number: 80/132.

Bryan, E. R. & Deakin, W. H. (1989) Tests and design of 175mm deep continuous and sleeved Zeta purlins. University of Salford, Department of Civil Engineering Report. Report number: J287.

Bryan, E. R. (1973) The Stressed Skin Design of Steel Buildings (Constrado Monographs). Crosby Lockwood Staples.

Davies, J. M. (1982) Manual of Stressed Skin Diaphragm Design. John Wiley & Sons Inc.

Hadjipantelis, N., Gardner, L. & Wadee, M. A. (2018) Prestressed cold-formed steel beams: Concept and mechanical behaviour. Engineering Structures. 172, 1057-1072.

Haidarali, M. R. (2011) Local and distortional buckling behaviour of cold-formed steel Z section beams. PhD thesis. Imperial College London, London, UK.

Haidarali, M. R. & Nethercot, D. A. (2011) Finite element modelling of cold-formed steel beams under local buckling or combined local/distortional buckling. Thin-Walled Structures. 49 (12), 1554-62.

Gorst, N. J. S., Williamson, S. J., Pallett, P. F. & Clark, L. A. University of Birmingham (ed.) (2003) Friction in temporary works. Birmingham, UK, Health and Safety Executive. Report number: 071.

Ho, H. C. & Chung, K. F. (2006) Analytical prediction on deformation characteristics of lapped connections between cold-formed steel Z sections. Thin-Walled Structures. 44 (1), 115-130.

Ho, H. C. & Chung, K. F. (2004) Experimental investigation into the structural behaviour of lapped connections between cold-formed steel Z sections. Thin-Walled Structures. 42 (7), 1013-1033.

Hui, C. (2014) Moment Redistribution in Cold-Formed Steel Purlin Systems. PhD thesis. Imperial College London.

Hui, C., Gardner, L. & Nethercot, D. A. (2016) Moment redistribution in cold-formed steel continuous beams. Thin-Walled Structures. 98 465-77.

Kyprianou, C., Kyvelou, P., Gardner, L. and Nethercot, D. A. (2018) Numerical Study of Sheathed Cold-Formed Steel Columns. 9th International Conference on Advances in Steel Structures, ICAAS'2018, December 5-7, Hong Kong, China.

Kyvelou, P., Gardner, L. & Nethercot, D. A. (2015) Composite Action Between Cold-Formed Steel Beams and Wood-Based Floorboards. International Journal of Structural Stability and Dynamics. 15 (8), 1540029 (17 pp.).

Kyvelou, P., Gardner, L. and Nethercot, D. A. (2017) Design of Composite Cold-Formed Steel Flooring Systems. Structures. 12, 242-252.

Kyvelou, P., Gardner, L. and Nethercot, D. A. (2017b) Testing and analysis of composite cold-formed steel - wood-based flooring systems. Journal of Structural Engineering. 143(11), 04017146 (16 pp.).

Kyvelou, P., Gardner, L. and Nethercot, D. A. (2018) Finite Element Modelling of Composite Cold-Formed Steel Flooring Systems. Engineering Structures. 158, 28–42.

Kyvelou, P., Hui, C., Gardner, L. and Nethercot, D. A. (2018b) Moment Redistribution in Cold-Formed Steel Two-Span Overlapped Purlin Systems. 8th International Conference on Thin-Walled Structures, ICTWS 2018, July 24-27, Lisbon, Portugal. Paper No:172.

Kyvelou, P., Hui, C., Gardner, L. and Nethercot, D. A. (2018c) Moment Redistribution in Cold-Formed Steel Sleeved and Overlapped Two-Span Purlin Systems. Advances in Structural Engineering. [in press]

Leach, P. (1990) Testing of 225 deep and 250 deep sleeved Zeta purlin systems. University of Salford, Department of Civil Engineering Report. Report number: J397.

Li, Z. & Schafer, B. W. (2010) Buckling analysis of cold-formed steel members with general boundary conditions using CUFSM: Conventional and constrained finite strip methods. 20th International Specialty Conference on Cold-Formed Steel Structures - Recent Research and Developments in Cold-Formed Steel Design and Construction, November 3, 2010 - November 4. 2010, St. Louis, MO, United states, University of Missouri-Rolla. pp.17-31.

Ortiz, F.J.M. (2018) The behaviour of cold-formed steel built-up structural members. PhD thesis. University of Sheffield.

Riks E. (1979) An incremental approach to the solution of snapping and buckling problems. International Journal of Solids and Structures. 15(7), 529-551.

Schafer, B. W., Li, Z. and Moen, C. D. (2010) Computational modeling of cold-formed steel. Thin-Walled Structures. 48 (10-11), 752-762.

Shifferaw Y., Vieira, Jr. L.C.M. and Schafer, B.W. (2009) Compression Testing of Single Column Studs with Sheathing Configurations. Department of Civil Engineering, Johns Hopkins University. Report.

Simaan, A. and Peköz, L. (1976) Diaphragm braced members and design of wall studs. Journal of the Structural Division, ASCE, 102(1), 77-92.

Telue, Y. and Mahendran, M. (2004) Behaviour and design of cold-formed steel wall frames lined with plasterboard on both sides. Engineering Structures, 26(5), 567-579.

Tian, Y.S., Wang, J. and Lu, T.J. (2007) Axial load capacity of cold-formed steel wall stud with sheathing. Thin-Walled Structures, 45(5), 537-551.

Yu, C. & Schafer, B. W. (2003) Local buckling tests on cold-formed steel beams. Journal of Structural Engineering. 129 (12), 1596-1606.

Vieira Jr. L.C.M., Shifferaw Y. and Schafer B.W. (2011) Experiments on sheathed cold-formed steel studs in compression. Journal of Constructional Steel Research. 67(10), 1554-1566.

Vieira, Jr. L.C.M. and Schafer, B.W. (2013) Behavior and design of sheathed cold-formed steel stud walls under compression. Journal of Structural Engineering, 139(5), 772-786.

Zhao, X. (2016) Measurement and Application of Geometric Imperfections in Cold-Formed Steel Members. PhD thesis. The Johns Hopkins University, Baltimore, USA.

LIST OF FIGURES

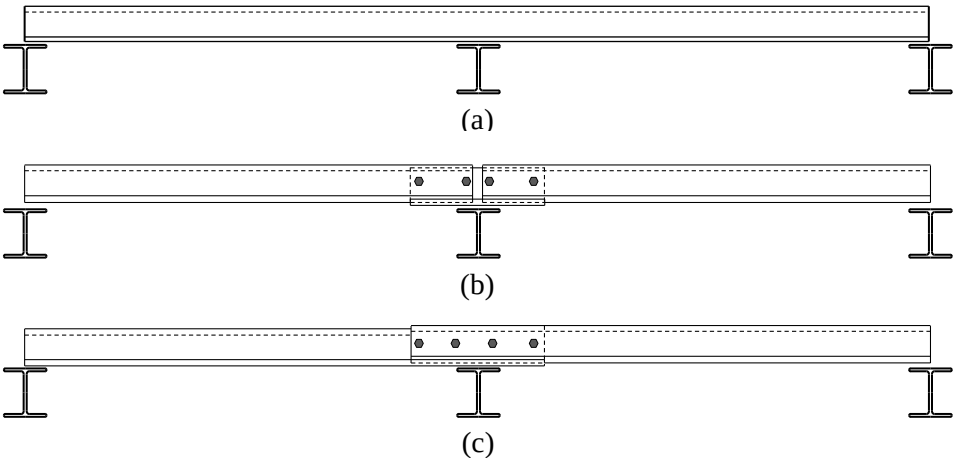

Figure 1: Two-span purlin systems: (a) bare, (b) sleeved and (c) overlapped (Kyvelou et al., 2018c)

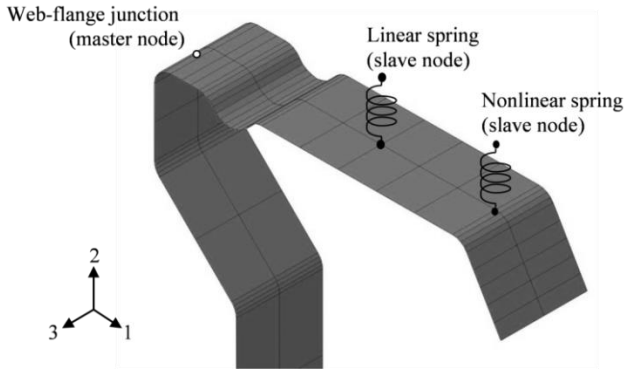

Figure 2: Two-spring model replicating profiled sheeting (Kyvelou et al., 2018c)

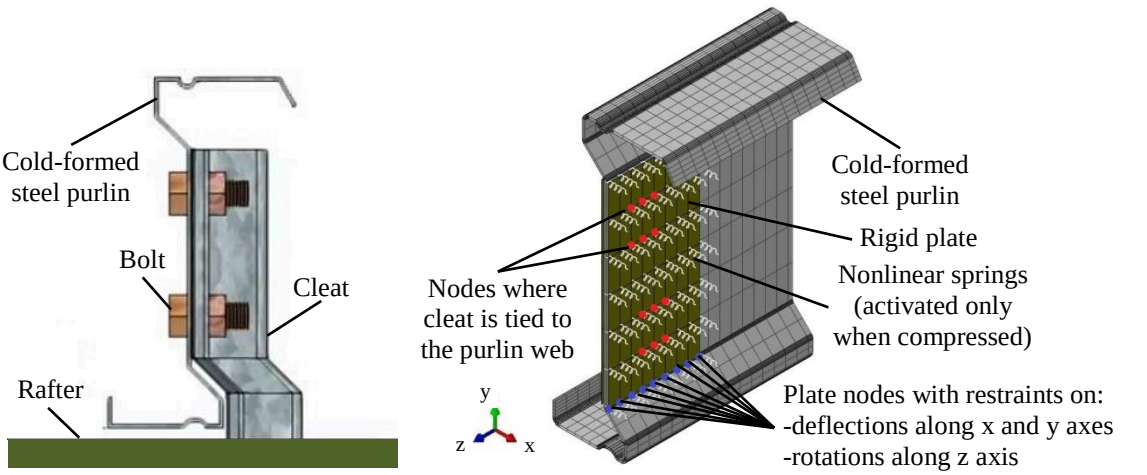

(a) Illustration of purlin supported by cleat (b) Numerical simulation of purlin-cleat connection

Figure 3: Numerical simulation of cleat supports

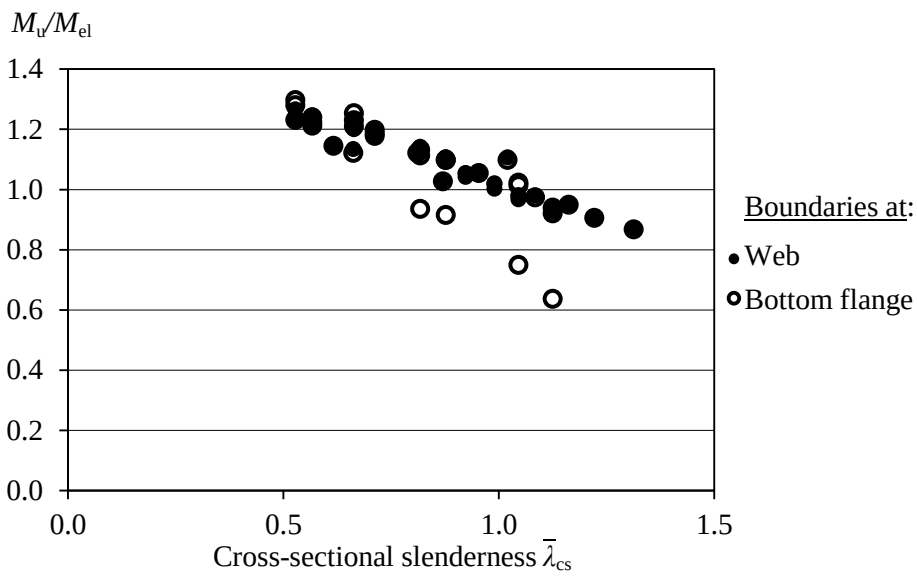

Figure 4: Influence of boundary conditions on the ultimate moment capacity of purlins with increasing slenderness

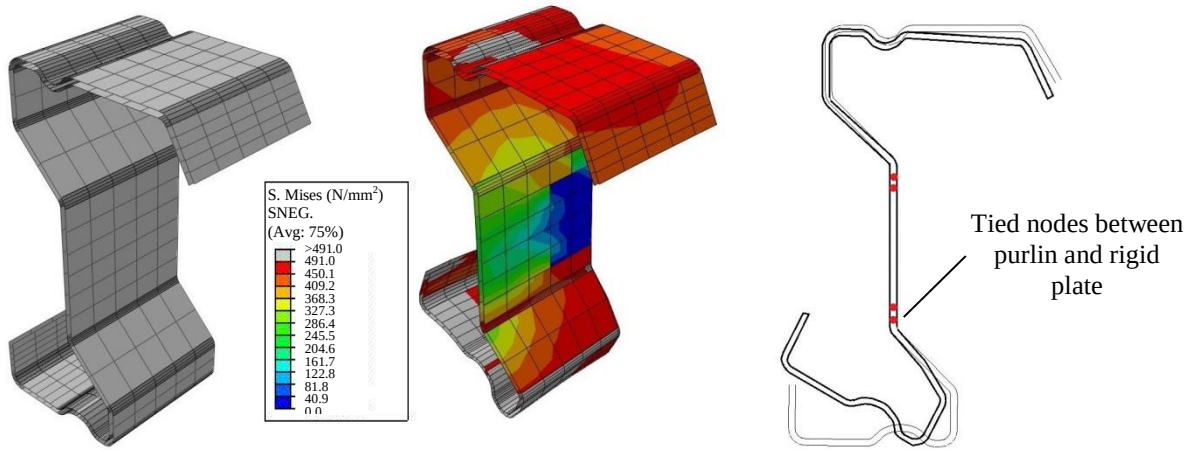

(a) Undeformed and deformed shape of central support region

(b) Undeformed and deformed cross-sectional shape

Figure 5: Lateral torsional buckling at the peak load of the system at the central support

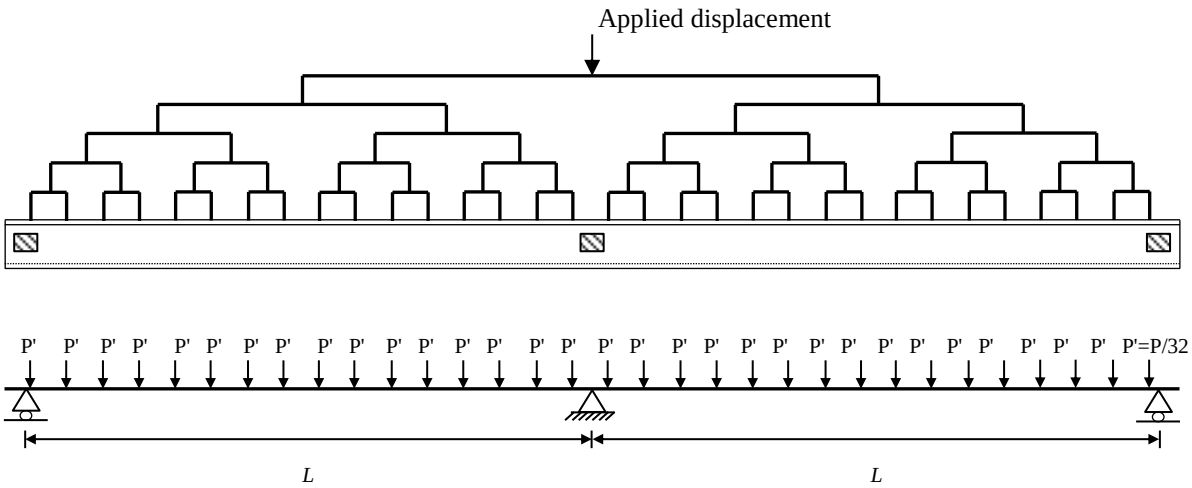

Figure 6: Whiffle tree developed for loading of the sleeved and overlapped two-span purlin systems (Kyvelou et al., 2018c)

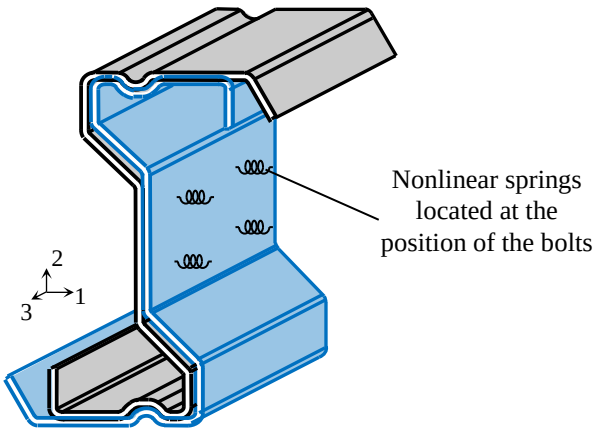

Figure 7: Numerical simulation of connection between purlins for sleeved and overlapped systems at the central support (Kyvelou et al., 2018b)

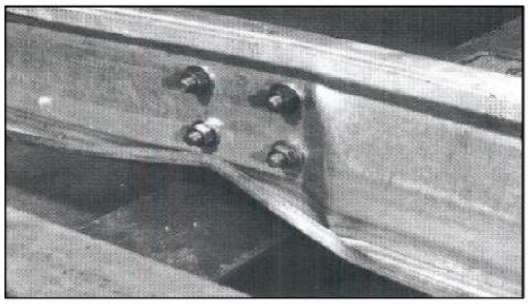

a)i. Test specimen (Yu & Schafer, 2003)

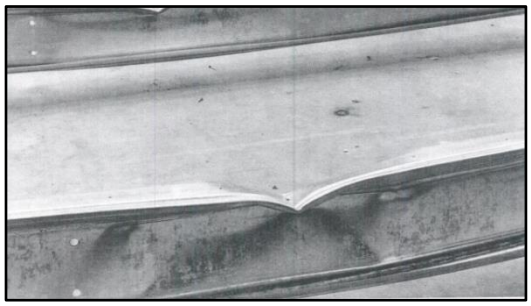

b)i. Test specimen (Leach, 1990)

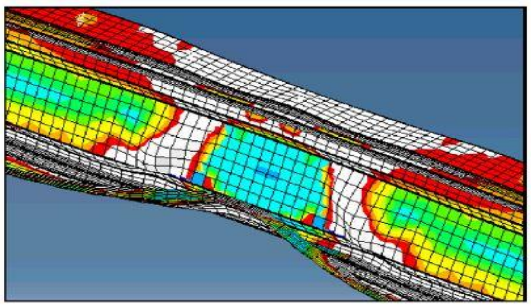

a)ii. FE model (Hui et al., 2016)

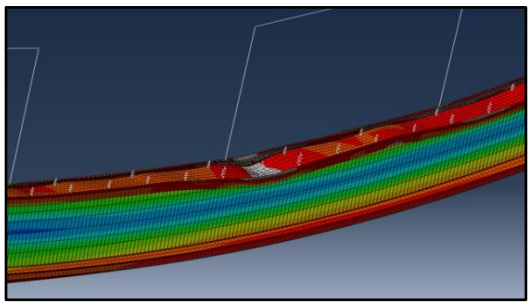

b)ii. FE model (Kyvelou et al., 2018b)

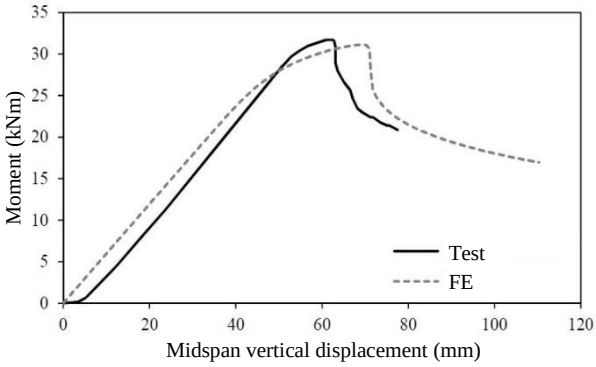

a)iii. Moment-vertical deflection response (Hui et al., 2016)

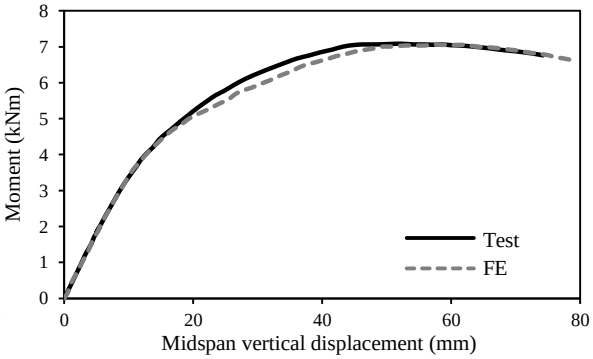

b)iii. Moment-vertical deflection response (Hui et al., 2016)

(a) Bare system

(b) Sleeved system

Figure 8: Comparison of failure modes and moment-vertical deflection curves between physical tests and FE models for (a) bare and (b) sleeved two-span purlins

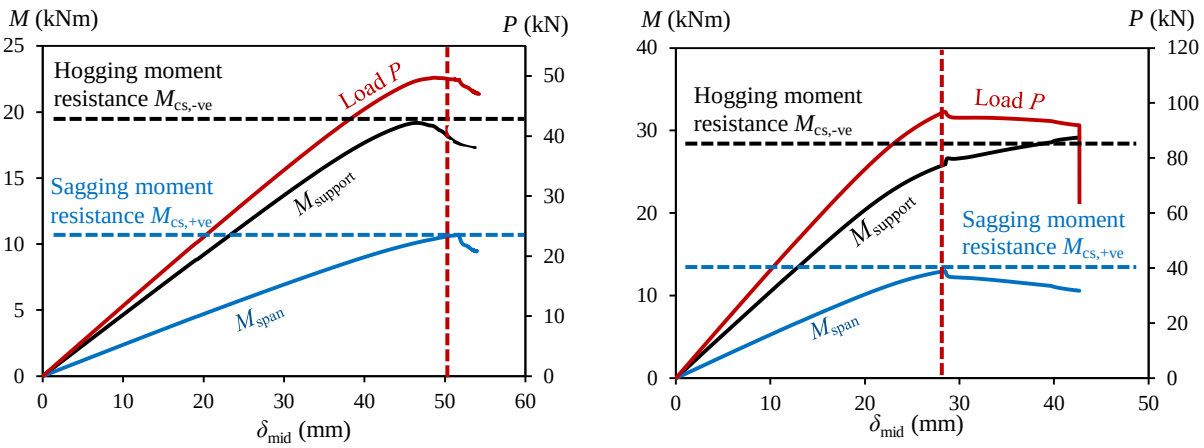

(a) Typical system with partial redistribution (b) Span-critical system with no redistribution

Figure 9: Observed structural responses of two-span purlin systems

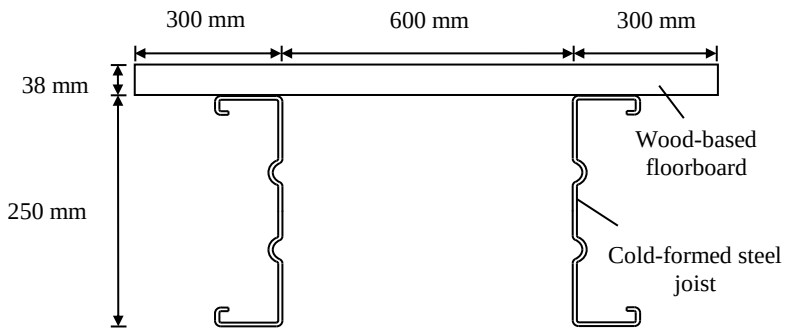

Figure 10: Typical cross-section of examined systems (Kyvelou et al., 2017b)

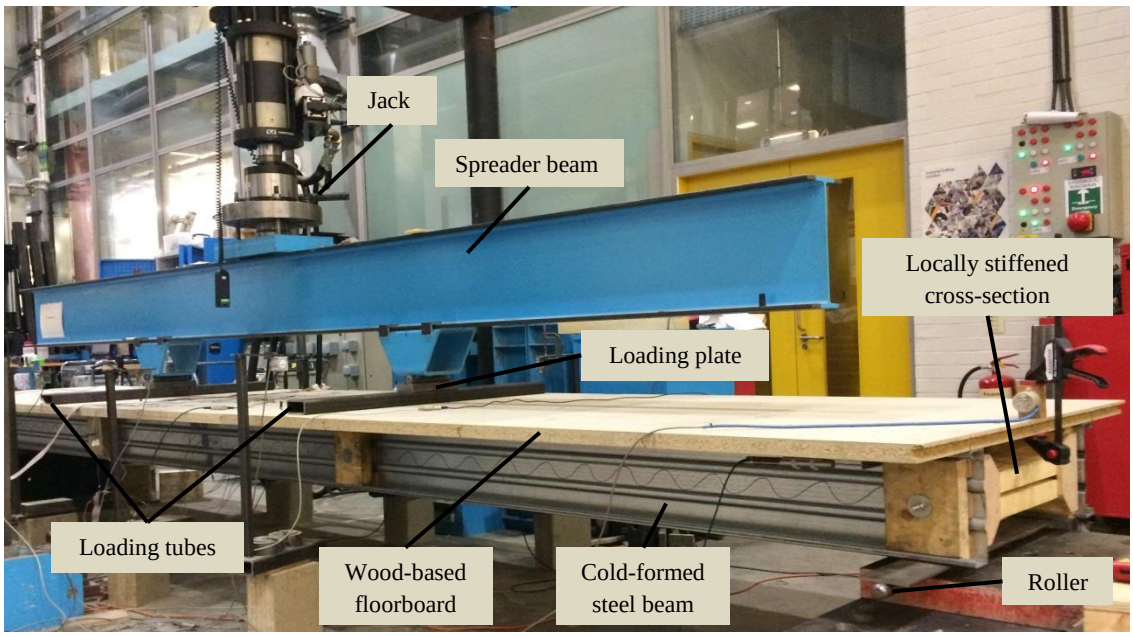

Figure 11: Experimental layout of composite beam tests (Kyvelou et al., 2017b)

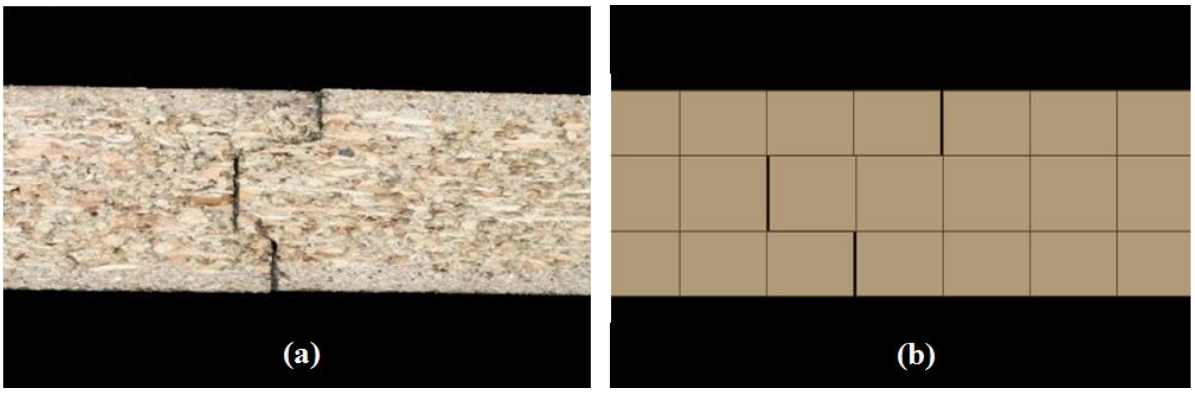

Figure 12: Gap between floorboards in (a) test and (b) finite element model (Kyvelou et al., 2018)

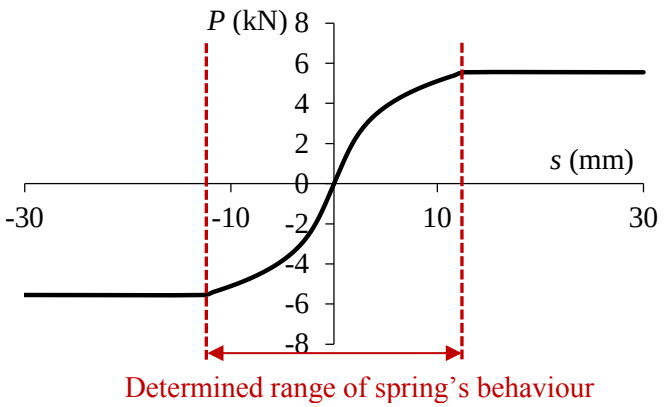

Figure 13: Load-displacement relationship assigned to nonlinear springs (Kyvelou et al., 2018)

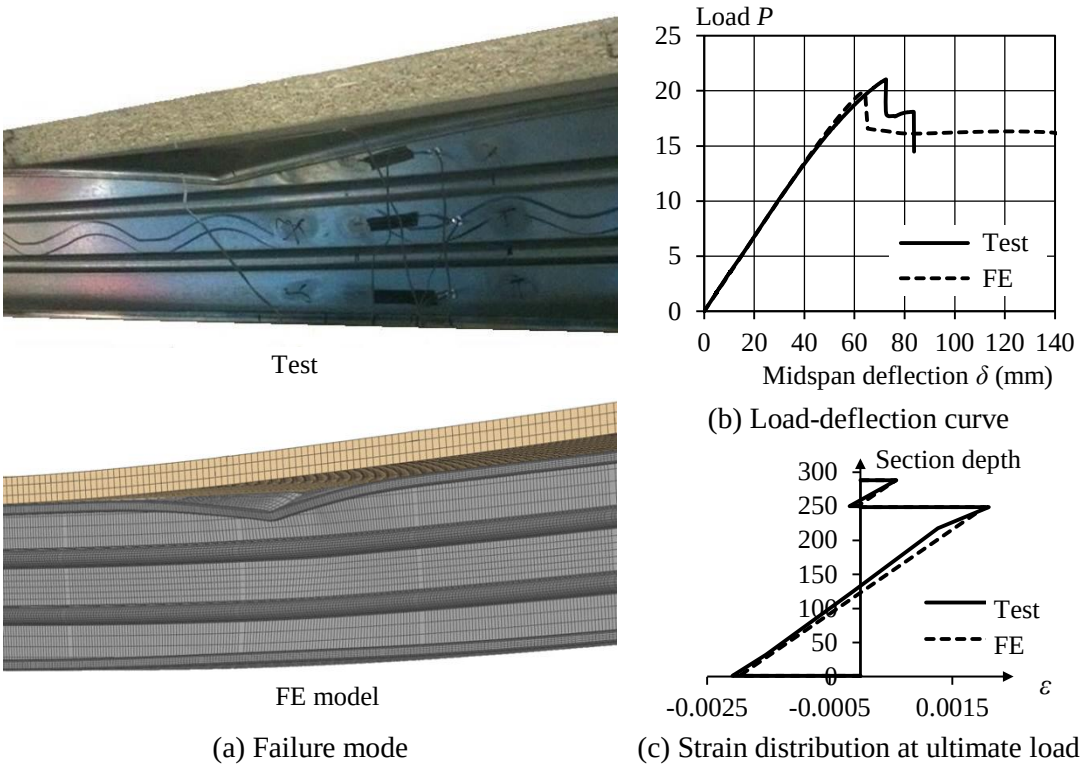

(a) Failure mode (b) Load-deflection curve (c) Strain distribution at ultimate load

Figure 14: Typical comparisons of (a) failure mode, (b) load-deflection curve and (c) strain distribution at ultimate load from physical test and numerical simulation (Kyvelou et al., 2018)

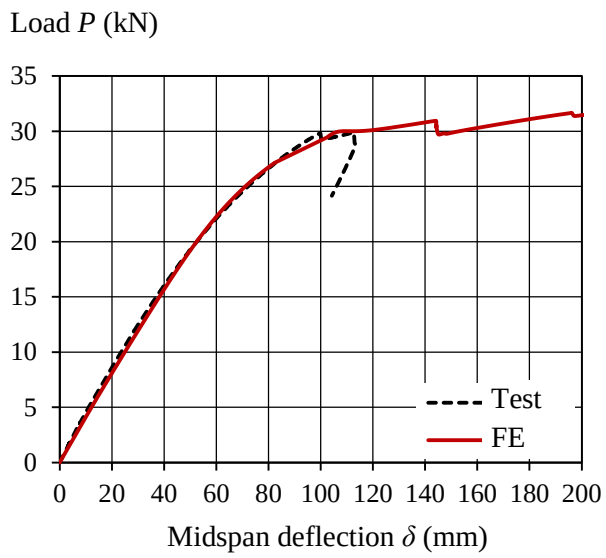

Figure 15: Comparison of load-deflection responses from test and numerical simulation for a typical specimen where the physical test was stopped prematurely (Kyvelou et al., 2018)

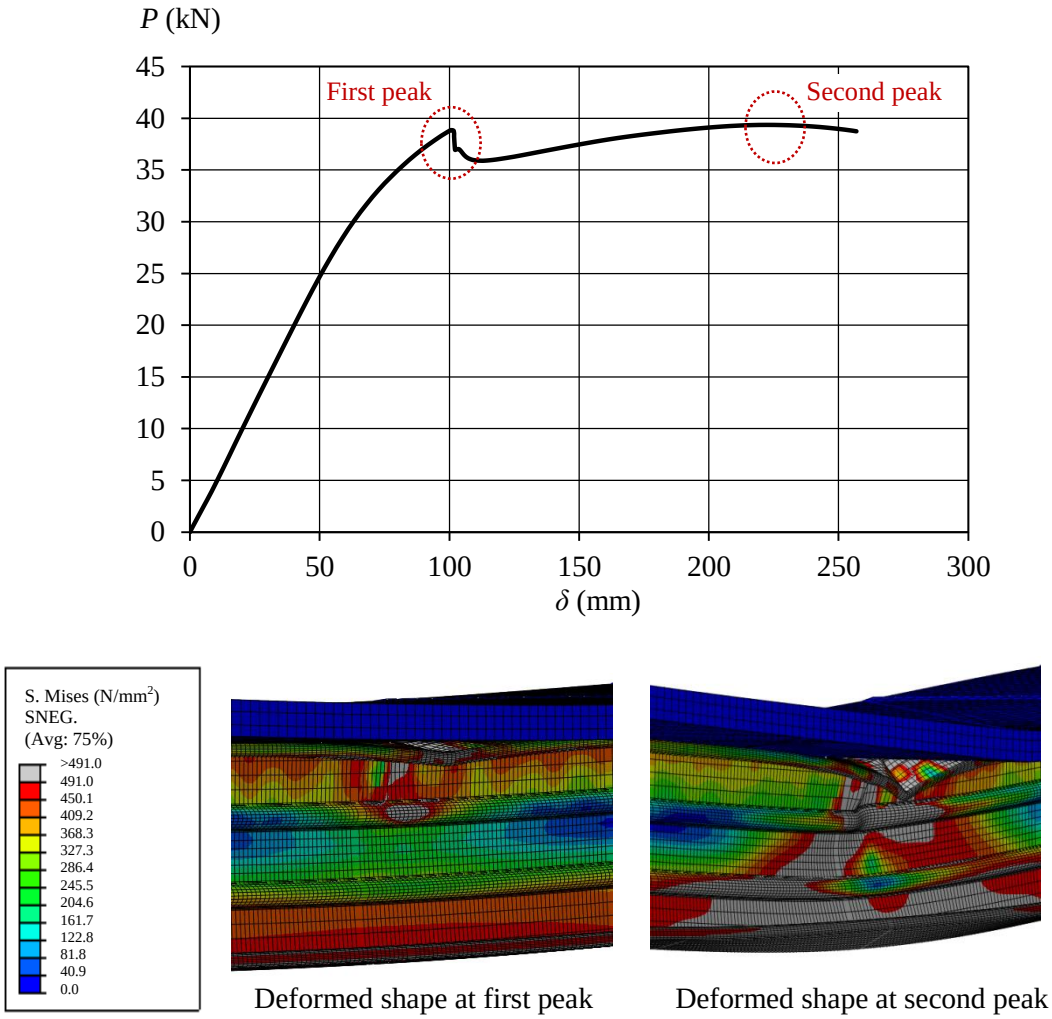

Figure 16: Typical load-displacement response exhibiting two peaks (Kyvelou et al., 2018)

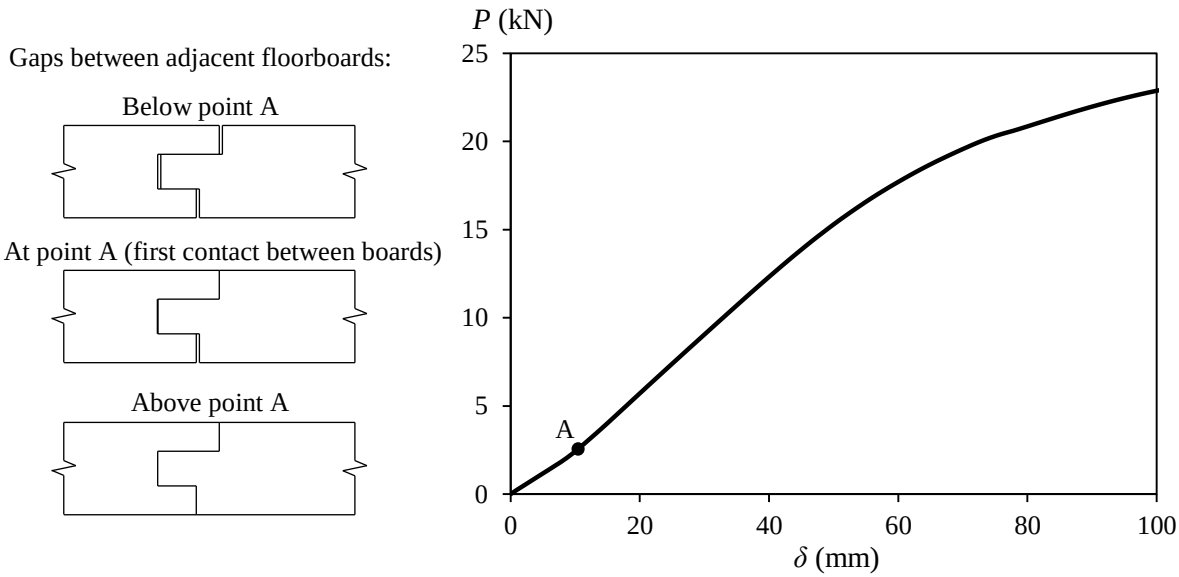

Figure 17: Change of slope of the load-deflection curve due to the closure of gaps between adjacent floorboards (Kyvelou et al., 2018)

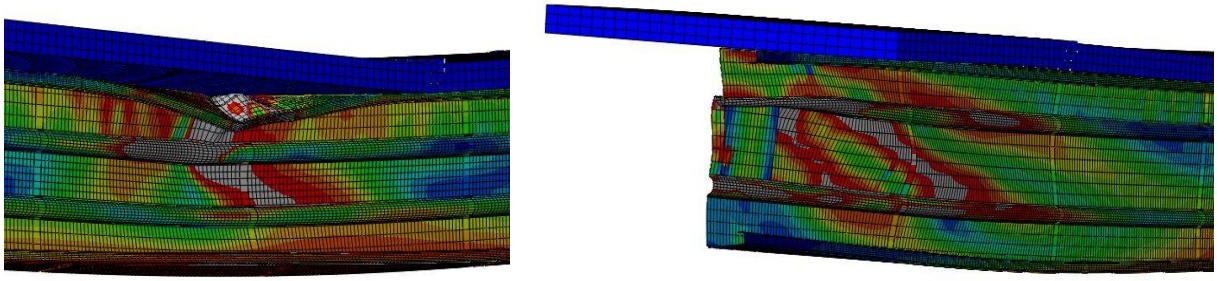

(a) Typical bending failure at midspan (b) Typical shear failure in shear span

Figure 18: Typical (a) bending and (b) shear failure (Kyvelou et al., 2018)

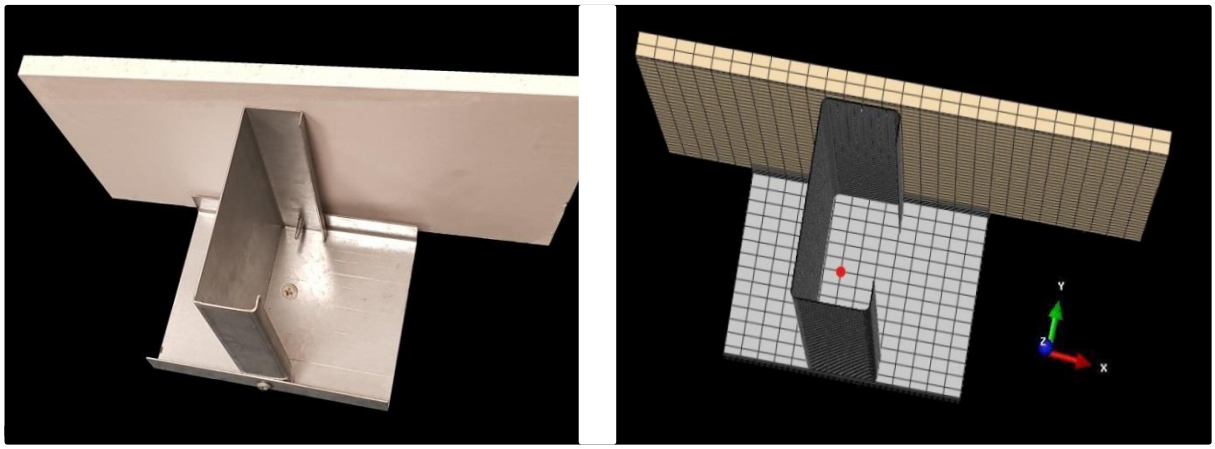

(a) Photograph of column-to-track connection (b) FE simulation of column-to-track connection

Figure 19: Column-to-track connection: (a) photograph and (b) numerical simulation

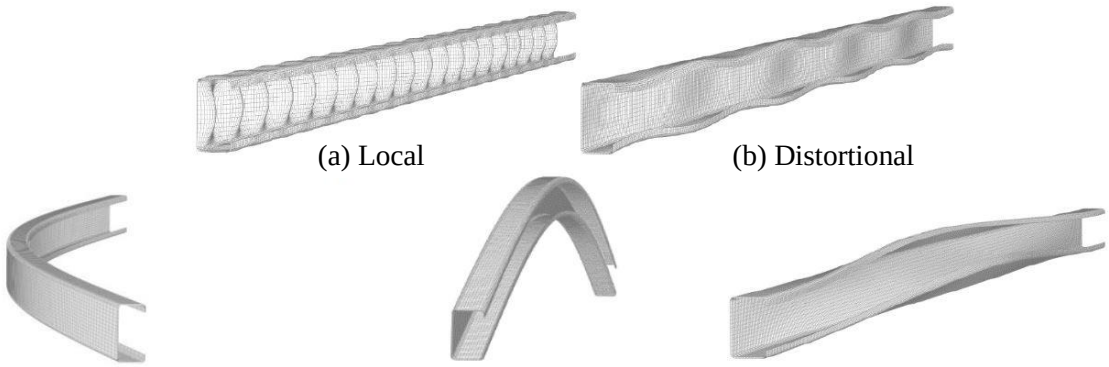

(a) Local (b) Distortional

(c) Minor flexural (d) Major flexural (e) Torsional

Figure 20: Longitudinal distribution of: (a, b) cross-sectional and (c-e) global imperfections (Kyprianou et al., 2018)

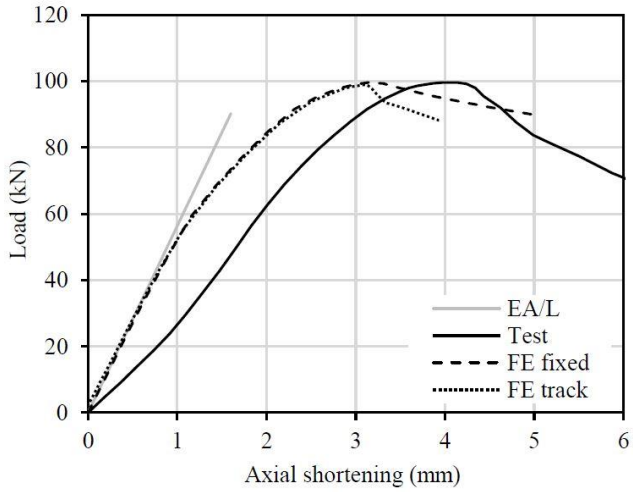

(a) Load-axial shortening curves

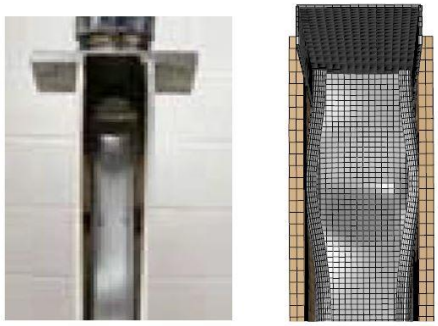

(i) Test (Shifferaw et al., 2009) (ii) FE model

(b) Failure modes

Figure 21: Typical comparisons between FE model and test specimen (Kyprianou et al., 2018)

LIST OF TABLES

Table 1: Summary of comparisons between finite element and test results

Test type	No. of tests	Mean $M_{u,FE}/M_{u,test}$	COV of $M_{u,FE}/M_{u,test}$
Single-span bare	45	1.00	0.04
Two-span bare	16	1.01	0.03
Single-span sleeved	34	1.00	0.07
Two-span sleeved	9	0.97	0.07
Single-span overlapped	19	1.01	0.08

Table 2: Summary of comparisons between finite element and 12 test results (Kyvelou et al., 2017b)

	$M_{u,FE}/M_{u,exp}$	$(EI)_{FE}/(EI)_{exp}$
MEAN	0.99	1.04
COV	0.05	0.05